International Journal of Mass Spectrometry 296 (2010) 30–35

Contents lists available at ScienceDirect

International Journal of Mass Spectrometry

journal homepage: www.elsevier.com/locate/ijms

Chirp dependent matrix-assisted laser desorption/ionization measurements of alkali metal adapted angiotensine II by using ultrashort laser pulses in the near IR regime

J.M. Wichmann*, F. Schwaneberg, C. Lupulescu, A. Lindinger

Freie Universität Berlin, Institut für Experimentalphysik, Arnimallee 14, 14195 Berlin, Germany

ARTICLE INFO

Article history:
Received 16 June 2010
Accepted 13 July 2010
Available online 5 August 2010

Keywords:
Angiotensine II
MALDI
Femtosecond laser technique 82.80.RT
82.53.−k
87.15.k

ABSTRACT

Matrix-assisted laser desorption/ionization (MALDI) with ultrashort laser pulses is reported in the near IR regime (central wavelength 800 nm). The used matrices show almost no absorption in this wavelength regime. This phenomenon is examined by applying different linear chirps leading to pulse durations up to several picoseconds and is compared with calculations based on a two photon transition. The results support the interpretation, that multiphoton absorption of the matrix molecules is a relevant factor by using ultrashort laser pulses. For characterization of the ionization process, the cationization and the fragmentation of the used analyte (angiotensine II) with potassium has been investigated in order to figure out the influence of the laser pulse properties. Thereto, the cationization and fragmentation tendency have been described in terms of laser pulse duration and energy.

1. Introduction

Matrix-assisted laser desorption/ionization (MALDI) is one of the most important tools to transfer non-volatile large molecules into the gas-phase [1–3]. In combination with time-of-flight (TOF) mass spectrometry, MALDI-TOF is a powerful technique in the field of biochemical and physiological research. The MALDI process itself is controversial and still an active field of research as recent publications show [4–6]. Several experimental and theoretical investigations indicated that MALDI can be described as a two step process [7,8]. In the first step, the laser pulse is absorbed by the matrix molecules and the desorption process occurs [9]. After photoresonant absorption of the laser pulse by the matrix molecules, the desorption process seems to be thermally driven. Direct photoresonant ionization of common used matrix molecules could not explain the ion formation completely due to the high ionization potential of comon matrix substances (about 8 eV) [7]. Referred to the model of R. Knochenmuss, photochemical and photophysical processes occure, e.g. pooling of excitons in order to ionize some matrix molecules leads to charge transfer from matrix molecules to the analyte. Simulations, using molecular dynamics (MD) methods by Knochenmuss and Zhigilei [10,11], in combination with charge transfer processes (described by a rate equation ansatz), give further evidence for the model, Knochenmuss and coworker described.

As mentioned, charge transfer is controversially discussed [7]. Two different models have been developed: The “cluster model” or “lucky survivor model” by Karas et al. [12] and the “pooling model” by Ehring et al. [13,7]. These models are in common, that the ionization process takes place after the desorption. In the cluster model ions are preformed and the separated cluster disintegrates into free ions. In the “pooling model”, charge transfer reactions from excited matrix molecules to the analyte take place in the gas-phase, the so-called MALDI plume. These gas-phase reactions have recently been described by using MD in combination with density functional theory (DFT) methods [14]. Reaction times for the complete MALDI process are several nanoseconds (ns) according to the described results of these theoretical and also experimental investigations [15].

MALDI matrix substances have absorption bands in the UV [16,17]. Therefore most commercial MALDI-TOF apparatuses use laser in the UV range (e.g. 337 nm for the common used nitrogen laser or 355 nm for a frequency-trippled Nd:YAG laser). These lasers have a laser pulse duration of a few nanoseconds. The absorption process has been examined with laser pulses of different wavelengths and the ion yield is strongly correlated with the absorption spectra of the used matrix substance. Common UV matrices absorb up to a wavelength of 430 nm [18]. MALDI experiments in the visible wavelength regime did not succeed with typical UV matrices. However, by using dye substances in polar solvents as matrices, MALDI takes place for wavelengths up to 532 nm, as reported in

* Corresponding author.
E-mail address: wichmann@physik.fu-berlin.de (J.M. Wichmann).

1387-3806/$ – see front matter © 2010 Elsevier B.V. All rights reserved.
doi:10.1016/j.ijms.2010.07.018

[19–21]. An important tool for the examination of the MALDI process is the variation of the laser pulse properties. Measurements with different wavelengths [22], pulse durations down to the ps time scale [23], and also two pulse measurements [24,25] have been reported in order to explain MALDI.

First MALDI experiments by using fs laser pulses in the near UV regime have been conducted by Papantonakis et al. [22] and Demirev et al. [26]. Their results show strong similarities in the obtained mass spectra. This result supports the idea of similarities in the MALDI processes for different pulse durations. Surprisingly, by using ultrashort laser pulses (on the fs timescale) MALDI processes occur in the near IR regime (800 nm), as recently reported [27], although the used matrix substances only have minor absorption in this wavelength regime [15,16].

In order to examine the charge transfer reactions, several experiments with different ions (protons, alkali ions) were performed for investigating the second step of the MALDI process, including cationization of peptides [28,29], oligosaccharides [30] and matrix substances itself [31] by using, e.g., potassium salts. Cationized peptides seem in several cases to be more stable in the MALDI process than their protonated molecules, especially for higher laser pulse energies [28,32]. Further investigations are protocols for special sample preparations in order to suppress cationized analyte peaks in mass spectra. Another reason for studying the cationization process is the mass and binding behavior of alkali ions compared to protonation.

In this work, MALDI measurements with ultrashort laser pulses in the near IR regime are presented. Since the early investiations of Weiner [33], it is known how to manipulate ultrashort laser pulses (in this wavelength regime) via spectral dispersion and recombination. Here we utilize a spatial light modulator (SLM), placed in the Fourier plane of the dispersed pulse to change the pulse duration via linear chirp.

In order to proof our interpretation, that MALDI with ultrashort laser pulses in the near IR regime is initiated by a multiphoton process, we examine the MALDI process with chirped laser pulses. In the first part, we compare the theoretically estimated dependency of the analyte ion signal on the laser pulse duration assuming a multiphoton absorption of the laser pulse. In the second part, a further examination of the cationization process is presented. Here, the influence of the laser pulse energy and the pulse duration on the cationization tendency is shown.

2. Experimental

This section contains three parts: the description of the laser setup with the production of the different pulse durations, the MALDI-TOF apparatus, and the routine of the measurement.

The laser system consists of a Ti:sapphire oscillator (based on a KAPTEYN-MURMANE design) seeding a multipass amplifier (Odin, Quantronix). This combination delivers 60 fs laser pulses with a central wavelength of about 800 nm with a repetition rate of 10 Hz. The maximal pulse energy is 1.3 mJ. By a gray-filter, the pulse energy is reduced to 0.25 mJ for remaining below the damage threshold of the liquid crystal modulator, which is sufficient for the MALDI experiments. The heart of this experiment is a spatial light modulator (SLM-640, CRI, Cambridge, MA, USA), consisting of two liquid crystal arrays of 640 pixels each. This SLM is centered in the Fourier plane of a zero dispersion compressor, which consists of two gold plated gratings of 1800 lines per mm and two cylindrical (silver coated) mirrors (f = 200 mm). This folded 4f-arangement is displayed in Fig. 1.

By applying a defined voltage on each pixel independently, it is possible to alter the second order phase up to 150,000 fs^2. This leads to a linear optical chirp and an increase of the time

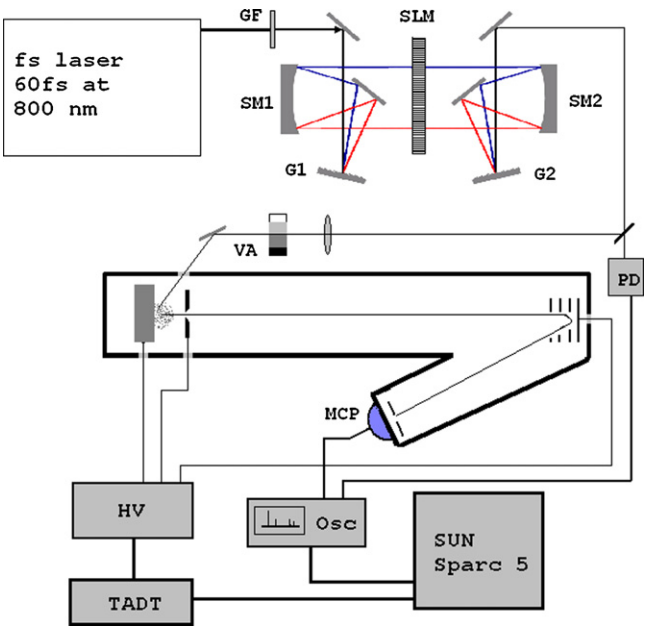

Fig. 1. A schematic view of the experimental setup. The fs laser pulses are created in the oscillator and amplified in a multipass laser amplifier. The grey-filter (GF) reduces the pulse energy to 0.25 μJ. The pulse duration is changed in the shaper setup, consisting of two gratings (G1 and G2), two cylindrical mirrors (SM1 and SM2), and a liquid crystal spatial light modulator (SLM), placed in the Fourier plane of the 4f-arrangement. After a variable attenuator (VA) the laser pulse is focused onto the sample holder. The created ions are accelerated with an electric field and mass analysed in a reflectron type of TOF. (HV denotes the high voltage power supply.) MCP denotes the multi channel plate and PD denotes the photo diode for triggering the oscilloscope (Osc). The interface between the MALDI-TOF and the SUN Sparc computer is the so-called TADT box.

duration of the laser pulse up to a duration of 6 ps. The pulse durations were measured by applying autocorrelation techniques (PulseCheck, APE, Germany). After recombination on the second grating, the laser pulse is focused with a lens system on the sample in the MALDI-TOF. The pulse energy is controlled via a variable attenuator and is measured before the entrance window of the vacuum system with a power meter (LaserMate, Coherent Inc., CA). For all mass spectrometric measurements, a modified MALDI-TOF (REFLEX, Bruker Daltonics, Bremen, Germany) was used. The modification is a dielectric mirror, placed to bring the fs laser pulses on the same optical path onto the sample holder (SCOUT26, Bruker Daltonics, Germany) as the common used nitrogen laser pulses. A closed-ciruit television (CCTV) camera (WV-CL 352, Panasonic, Germany) controls the exact position and diameter of the laser pulse on the surface of the sample holder. The produced ions were accelerated by an electric field, created by the MALDI target and a second electrode nearby. The acceleration voltage was 24.17 kV. The ion beam is focused by an electric lens and enters the reflectron type of TOF and is detected by a multichannel plate. Data acquisition was performed by using a 1 GHz oscilloscope (LSA 1000, LeCroy, Chesnut, NY, USA) and a workstation (Sparc 5, Sun Microsystems, CA, USA). The built-in microcontroller governs the complete measurement via the commercial software package (XACQ 4.01, Bruker Daltonics, Germany). The mass spectra were analyzed by the computer program flexAnalysis 2.0 (Bruker Daltonics, Germany).

All used chemicals for the sample preparation (3,5-dimethoxy-4-hydroxycinamic acid (sinapic acid, SA), α-cyano-4-hydroxycinamic acid (CHCA), acetonitrille (ACN), triflouroacetic acid (TFA), angiotensine II (Ang), and potassium chloride (KCl)) were purchased from Fluka (Buchs, Switzerland) and used without further purification. The matrix solution contains 12 mg/ml CHCA, 12 mg/ml SA, 0.1% TFA solved in 1:1 ACN/distilled water and was

stirred for about one hour due to the poorly solvable matrix substances. This combination of CHCA and SA ensures that all cationized mass peaks are visible in the mass spectrum by using fs laser pulses in the near IR regime. Also, this combination creates the highest ion yield for laser pulses in the near IR regime. By using only CHCA as matrix substance, most of the cationized analyte peaks are suppressed in the MALDI mass spectra for lower laser pulse energies. Another important advantage is the smooth (white-shining) surface of the sample. This leads to a better signal-to-noise ratio of 15–20%, using fs laser pulses. The peptide (Ang) and, in case of examinations of the cationization process KCl are solved in distilled water as well (about 10 μg/ml). Angiotensine II is a good candidate, because its protonated mass (about 1047) is separated from fragment and matrix peaks (m/z below 400). The second advantage is the good proton/cation affinity of angiotensine II. For sample preparation, 1.2 μl matrix solution is mixed with a 1:1 combination of the peptide solution and the salt solution on the sample holder. For the proof of the multiphoton absorption/ionization thesis, 1.2 μl of the peptide solution (without KCl) was given onto the sample holder. Afterwards, the sample was dried in the fume hood at room temperature for two hours. This sample preparation method ensures a high sample thickness in order to make sure most of the laser pulse energy is absorbed by the MALDI sample. For one mass spectrum, the sum of two hundred laser shots was added. During the measurements, the sample target was continuously moved in order to average out over the exposed surface and to avoid irradiating black or hot target spots. Measurements were performed at least six times for a better signal-to-noise ratio. The mass spectra were smoothed and base-line subtracted by using the flexAnalysis (Version 2.0, Bruker Daltonics, Germany) program package.

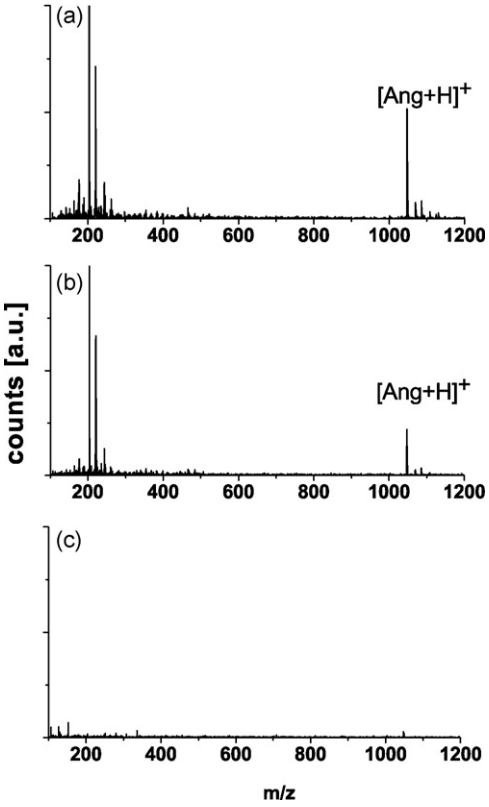

Fig. 2. MALDI mass spectra of angiotensine II by using fs laser pulses of a central wavelength at 800 nm. The pulse energy was constant at $E = 30$ μJ. The chirp values lead to pulse durations between 120 fs (for no chirp, spectrum (a)), 600 fs (for a chirp of 30,000 fs^2, spectrum (b)), and 6 ps (for 100,000 fs^2, spectrum (c)). The peak intensities of the analyte peaks become significantly lower for higher chirp values (respective higher pulse durations). Also the matrix and fragment peak intensity decreases for higher pulse durations.

3. Results and discussion

This section consists of two parts. In the first part, a proof of the multiphoton absorption is given by comparing theory with the measured ion yield of the MALDI process. In the second part, further examinations on the cationization process of peptides (with potassium) in the MALDI process will be shown and discussed.

3.1. Proof of the multiphoton absorption assumption

The new phenomenon of MALDI working also in the near IR regime with standard UV-MALDI matrices was interpreted as multiphoton absorption [27]. In order to proof this thesis, different pulse durations up to a few ps have been generated by linear chirps.

With these laser pulses in the near IR regime, the MALDI process has been performed. MALDI mass spectra for different values of linear chrips are shown in Fig. 2. The spectra reveal that the higher the chirp values (higher pulse durations), the lower the peak intensities of the analyte peaks. As a qualitative measure for the laser pulse absorption, the analyte ion yield ([Ang+H]$^+$) has been used. In order to change the pulse duration, the linear chirp has been modified. In the range up to 40 μJ laser pulse energy, the analyte peak intensity rises and fragmentation seems not to be a relevant factor. As described in common laser physics textbooks, different pulse durations can be produced out of an ultrashort laser pulse (the unchirped pulse duration is denoted as τ_0) by a linear chirp C.

$$\tau = \tau_0 \cdot \sqrt{1 + \frac{16 \cdot (2 \ln 2)^2 \cdot C^2}{\tau_0^4}}$$

This is in good agreement with the measured pulse durations. Two photon absorption (TPA) as a function of the pulse duration can be described by introducing $\mathrm{TPA} \propto I^2 \cdot \tau$. Using the laser pulse intensity $I \propto E/\tau$ leads to $\mathrm{TPA} \propto E^2/\tau$. Hence, for constant laser pulse energy TPA can be expressed by β/τ, where β is a scaling parameter. For accurate determination of the two photon absorption, the recorded experimental values of $\tau(C)$ have been used. In order to compare the measured peak intensities with the theoretical absorption TPA for different pulse durations, a χ^2-minimization has been performed with only β as the scaling parameter. The direct comparison of the peak intensities as function of the linear chirp is presented in Fig. 3(a). The measured peak intensities are in good accordance to the theoretical curve, as shown in Fig. 3(b). For the presented experimental results, the unchirped pulse duration after the SLM modulator setup was about 120 fs (measured by autocorrelation). The pulse energy was chosen to 30 μJ in order to minimize noise and fragmentation. For lower pulse energies, the signal-to-noise ratio of the ion yield decreases, and for higher pulse energies (over 40 μJ), fragmentation of the analyte becomes more relevant, especially for short pulse durations (up to 300 fs). The good agreement of the theoretical curve and the measured data could be seen as a proof for the idea that MALDI in the near IR regime for ultrashort laser pulses can be described by two photon absorption of the matrix. By using fs laser pulses with a central wavelength of 800 nm, the analyte ion yield is much more noisy compared to wavelengths in the UV due to faster sample degregation. Because of the high thickness of the MALDI sample, there is no iron mass peak visible in the MALDI mass spectra. This indicates no ablation of the sample holder for laser pulse energies up to at least 100 μJ.

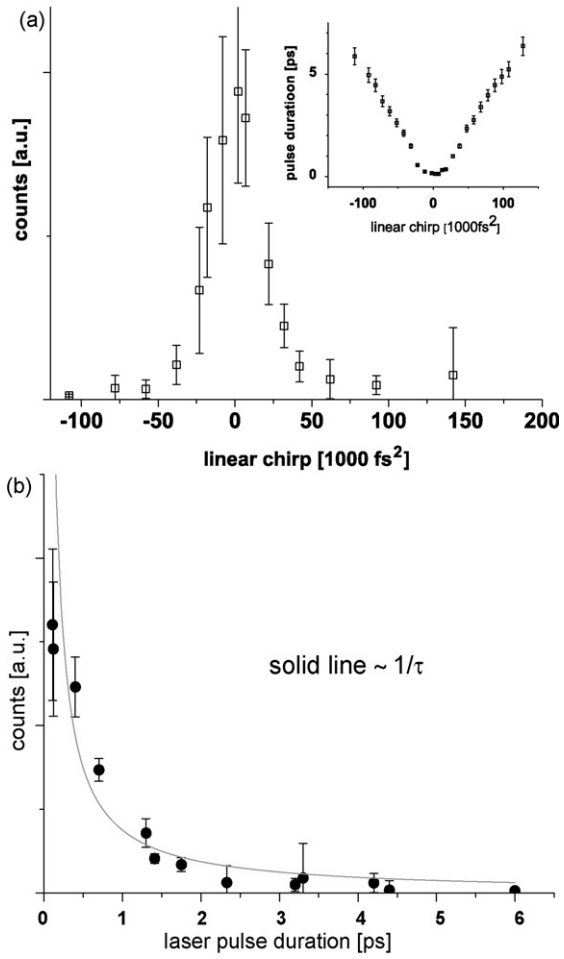

Fig. 3. (a) Direct comparison of the $[Ang+H]^+$ peak intensity [■] as a function of the linear chirp. The inset shows the measured laser pulse duration as a function of the linear chirp. (b) The analyte ion yield as a function of the measured laser pulse duration. The solid line represents the β/τ fit. The pulse energy was constant at $E = 30\ \mu J$. The error bars represent the standard deviations of the five single measurements.

3.2. The cationization process

The phenomenon of cationization of angiotensine II was recently reported for fs and ns laser pulses in the UV regime [32]. Here, further results by using fs laser pulses with a central wavelength of 800 nm for different pulse durations and pulse energies are presented. The results are qualitatively similar for the cations sodium, potassium, rubidium, and caesium. In this work, results of potassium are presented, because these measurements show the best signal-to-noise ratio of all measured data. As mentioned in the experimental section, a high concentration of potassium ions has been brought into MALDI by adding a small amount of KCl into the aqueous sample. By using fs laser pulses with a central wavelength of 800 nm, the cationization tendency of angiotensine II could be examined by varying the pulse duration and the pulse energy. The cationization tendency was measured by the ratio of the peak intensities [Ang+K]/[Ang+H]. This ratio decreases for higher laser pulse durations (at constant laser pulse energy) and increases for higher laser pulse energies (at constant laser pulse durations), respectively (see Figs. 4 and 5). However, for higher laser pulse energy (over about 30 μJ) at low pulse durations (up to 300 fs), fragmentation of all analyte species becomes a relevant factor. The fragmentation shows a different behaviour with respect to the laser pulse parameters for [Ang+H] and [Ang+K] (see Figs. 4 and 5). Cationized angiotensine II seems to be more stable than [Ang+H] when

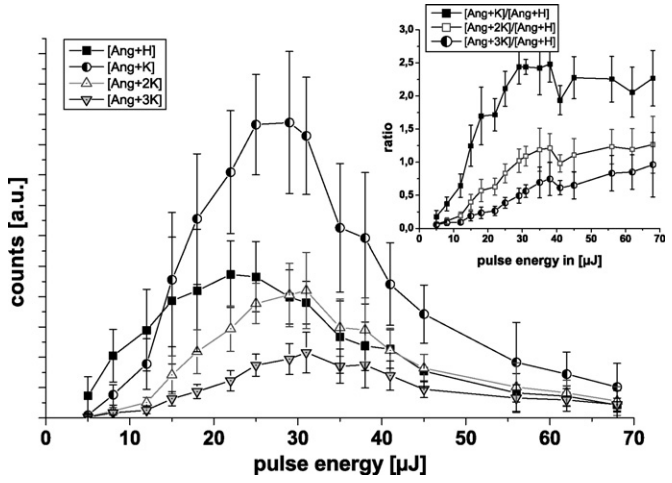

Fig. 4. In this diagram, the peak intensities of the protonated and potassium adapted angiotensine II peaks are shown for different laser pulse energies. The central wavelength was about 800 nm and the laser pulse duration 70 fs. In the inset, the ratio of the peak intensities is presented. The ratio increases for higher laser pulse energies and becomes constant for pulse energies larger than about 30–40 μJ due to fragmentation.

irradiating with high pulse energy. This is in common with results by Freeke et al. showing that attached counter ions could stabilize peptides in the gas-phase [32].

Figs. 4 and 5 present the experimental results of the discussed measurements. The peak intensities of protonated and cationized angiotensine II are shown as functions of the laser pulse energy (for constant pulse duration of 70 fs) and the pulse duration (for constant pulse energy of 55 μJ). The ratio [Ang+K]/[Ang+H] indicates the cationization tendency. The ion yield as a function of the laser pulse parameters is different for protonated and cationized angiotensine II (see Figs. 4 and 5). Uncertainties of potassium chloride or angiotensine II concentration of the sample lead to a low signal-to-noise level, especially for low laser pulse energies. Furthermore, the peak intensity of the higher cationized species

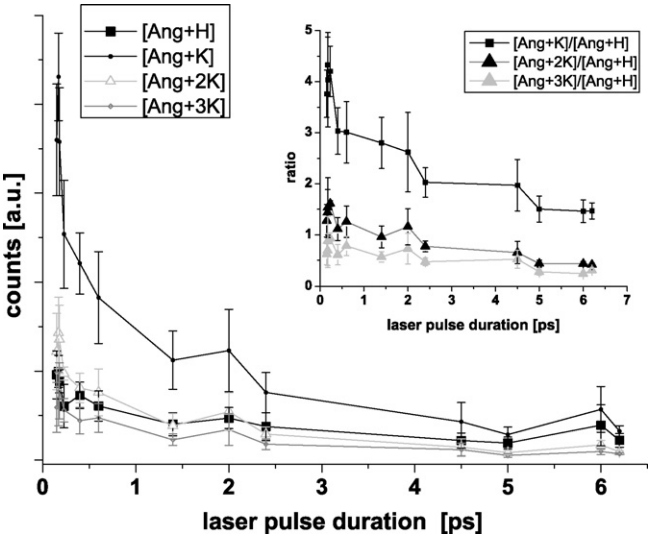

Fig. 5. Peak intesities of protonated and potassium adapted angiotensine II. The laser pulse energy was constant at $E = 55\ \mu J$. $[Ang+K]^+$ is always the highest peak in the spectrum, if KCl was added to the sample and ultrashort laser pulses with a central wavelength of $\lambda = 800$ nm have been used. The signal-to-noise ratios of the higher cationized species ($[Ang+2K-H]^+$ and $[Ang+3K-2H]^+$) are lower than the protonated and the single cationated ones in the MALDI mass spectra. The inset shows the cationization tendency (ratios of the peak intensities) as a function of the laser pulse duration.

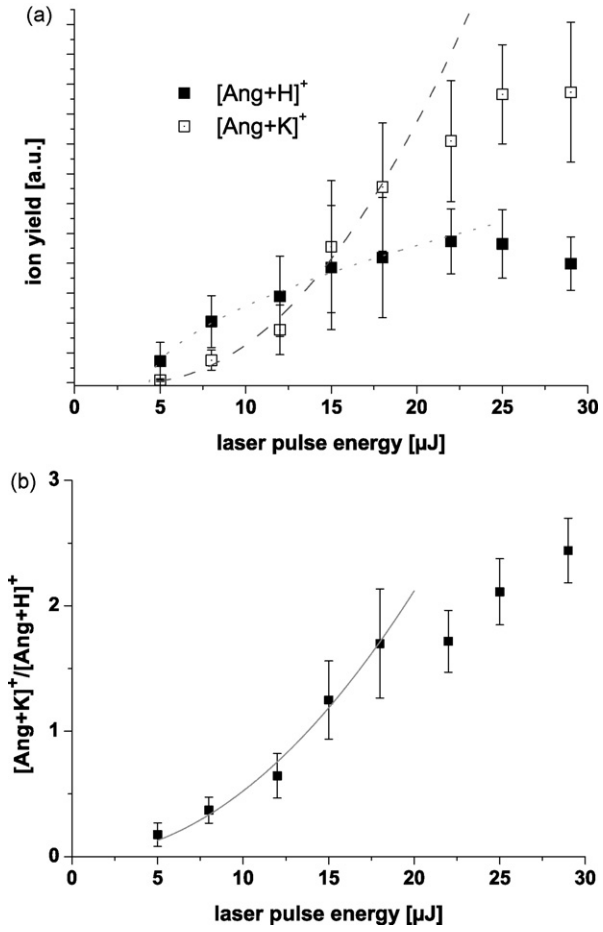

Fig. 6. (a) The protonated (⊡) and the cationized (■) angiotensine II peak intensities as a function of the laser pulse energy. The fit curve is only valid up to a laser pulse energy of 20 µJ. The dashed and dotted lines represent the fitted curves respectively. (b) Combination of these peak intensities as ratios as a function of the laser pulse energy. The solid line is the fitted curve E^A (described in the text). The error bars represent the standard deviations.

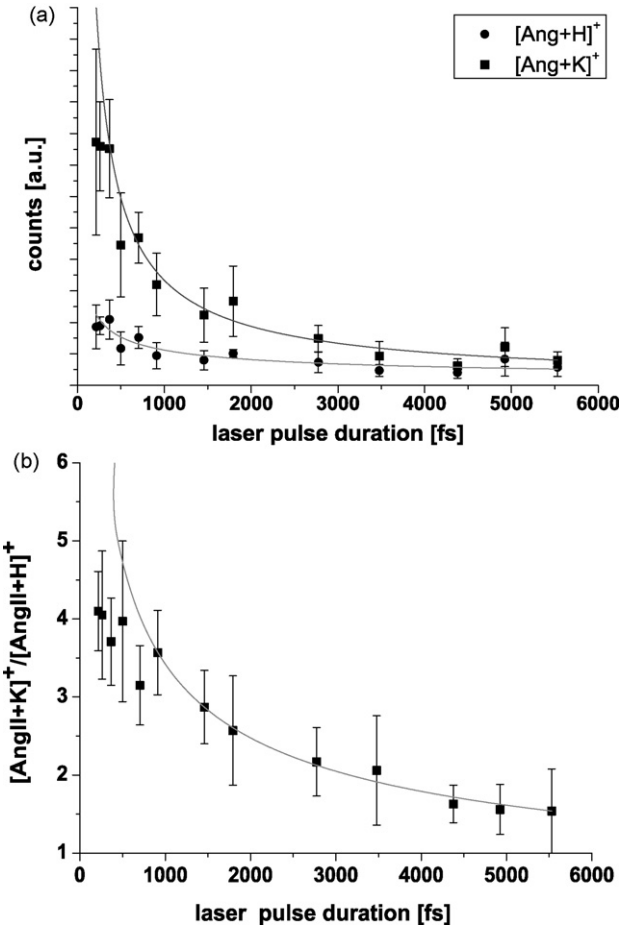

Fig. 7. (a) The analyte peak intensities as a function of the laser pulse duration. The laser pulse energy was chosen to $E = 55$ µJ. (b) The ratio of the peak intensities. A constant ratio regime for low pulse durations (below 1 ps) is visible, probably due to fragmentation. For higher laser pulse durations, fragmentation seems not to be a relevant factor (as the decrease of the ratios suggests). The error bars represent the standard deviation and the solid lines the fit curves $[\text{Ang+X}] \propto \tau^a$ (for A) $[\text{Ang+K}]/[\text{Ang+H}] \propto \tau^B$ (for B), as described in the text.

([Ang+2K], [Ang+3K]), especially for higher laser pulse durations is too low for further quantitative data analysis. Hence, in this work, only [Ang+H] and [Ang+K] peak intensities were analyzed. For the chosen potassium concentration in the MALDI sample, neither the [Ang+H] nor the [Ang+K] peak intensity as a function of the laser pulse duration are clearly proportional to $1/\tau$. The cationization process is still under debate. Particulary the dependence of the signal intensity on the laser pulse parameters (energy and duration) will be investigated. For these examinations, the peak intensities ([Ang+X], X = H, K) are the measures of the laser pulse absorption. The single peak intensities as well as the cationization tendency could be quantified as $[\text{Ang+X}] \propto I^n \tau^m$. This leads to $[\text{Ang+X}] \propto E^n \tau^{m-n}$. In order to separate the single fit procedures, we denote in case of the peak intensities $m := a_X$, $m - n := b_X$ and for the cationization tendency, $m := A$ and $m - n := B$. The influence of the laser pulse energy and the fit curve is shown in Fig. 6. The result of the fit procedure is $a_H = 0.57 \pm 0.2$ and $a_K = 2.05 \pm 0.9$ for a constant laser pulse duration of 70 fs. In the low pulse energy regime, the cationization process should not be influenced by fragmentation and other processes. Hence, 20 µJ for the upper limit in the fit procedure have been chosen. The influence of the laser pulse duration for constant laser pulse energy of 55 µJ is shown in Fig. 7(b). The fit procedures quantify $b_H = -0.45 \pm 0.17$ and $b_K = -0.85 \pm 0.1$ leading to $m_H = 0.12 \pm 0.25$ and $m_K = 1.2 \pm 0.9$. The cationization tendency as a function of the laser pulse energy is shown in Fig. 6(b). The result of the fit procedure is $A = 2 \pm 0.2$ by using energy values up to 20 µJ. As a function of the laser pulse duration (see Fig. 7(b)), the cationization tendency has been figured out to $B = 0.47 \pm 0.1$. As visible in Fig. 7, fragmentation is relevant in this pulse energy regime up to pulse durations of $\tau = 1$ ps. Hence, pulse durations from 1 to 6 ps have been chosen for the fit procedure.

The values af A and B should be more representative than a and b, because pulse-to-pulse and spot-to-spot uncertainties (e.g., hot-spots) are cancelled out due to ratio formation. The numerical result of A is strongly correlated to the range of laser pulse energies. Figs. 6 and 7 show that the chosen pulse energy and the duration regimes have a great influence on the fit result. Hence, these measurements and data analysis lead to $[\text{Ang+K}]/[\text{Ang+H}] \propto E^{2\pm0.2}/\tau^{0.5\pm0.1}$. A higher pulse energy regime (e.g., from 15 to 30 µJ) could also suggest a linear increase of τ as a function of the pulse energy. However, MALDI measurements are performed in the low pulse energy regime (about 10–20 percent above the pulse energy threshold) and the laser pulse energy range is chosen up to 20 µJ in order to suppress any fragmentation effect. It should be pointed out that we observe no quadratic pulse energy behavoir for [Ang+H] in the presence of potassium cations in the MALDI sample. This indicates a cationization mechanism in the plume during the MALDI process since fragmentation does not occur in the low laser pulse energy regime (see Fig. 3). As mentioned in the introduction, the theory of charge transfer in

MALDI is still controversial. Recent reports [34,35] interpret the Matrix Suppression Effeft, that the "cluster model" of Karas et al. could also contribute to MALDI. But our experimental results on cationization suggest that charge transfer in the gas-phase is still a relevant factor, because the cationization tendency due to the cluster model should not be influenced that strong by varying the laser pulse parameters. These experimental results could also help to proof a theory or a calculation. In order to figure out the proton or cation affinities of the used matrix substances or angiotensine II, these measurements could also be the empirical part.

4. Conclusion

In this work, we presented experimental results which support the idea, MALDI by using femtosecond laser pulses in the near IR regime works because two photon absorption is a relevant factor for energy deposition in the matrix. Furthermore, the catonization tendency [Ang+K]/[Ang+H] have been measured and validated for different energies and duration values of the laser pulse. These experiments suggest for a central wavelength of $\lambda = 800$ nm, that [Ang+K]/[Ang+H] increases as a function of the laser pulse energy almost quadratic and decreases for an increase of the pulse duration by the power of 0.5 ± 0.1 in the low laser pulse intensity regime. These dependencies are now available for a comparison with theoretical calculations. Now, further investigations could explain these phenomena and help to understand charge transfer processes in MALDI.

Acknowledgements

The authors would like to thank F. Weise, and O. Gause for their help to run the LabView program, L. Wöste for fruitful discussions, and the Deutsche Forschungsgemeinschaft (SFB 450) for financial support.

References

[1] M. Karas, D. Bachmann, F. Hillenkamp, Influence of the wavelength in high-irradiance ultraviolet laser desorption mass spectrometry of organic molecules, Anal. Chem. 57 (1985) 2935–2939.
[2] M. Karas, D. Bachmann, U. Bahr, F. Hillenkamp, Matrix-assisted ultraviolet laser desorption of non-volatile compounents, Int J. Mass Spectrom. Ion Process. 78 (1987) 53–68.
[3] M. Karas, F. Hillenkamp, Laser desorption ionization with molecular masses exceeding 10000 Daltons, Anal. Chem. 60 (1988) 2299–2301.
[4] R. Knochenmuss, A biopolar rate equation model of MALDI primary and secondary ionization processes, with application to positive/negative analyte ion ratios and suppression effects, Int. J. Mass Spectrom. 285 (2009) 105–113.
[5] F. Hillenkamp, Positive and negative ion yield in matrix-assisted laser desorption/ionization revisited, Int. J. Mass Spectrom. 285 (2009) 114–119.
[6] E.E. Durrant, R.S. Brown, Wavelength dependence on the level of post-source metastable ion decay observed in infrared matrix-assisted laser desorption ionization, Int. J. Mass Spectrom. 287 (2009) 119–127.
[7] R. Knochenmuss, Ion formation mechanisms in UV-MALDI, Analyst 131 (2006) 966–986.
[8] M.E. Belov, C.P. Myatt, P.J. Derrick, Chemical ionization of neutral peptides produced by matrix-assisted laser desorption, Chem. Phys. Lett. 284 (1998) 412–418.
[9] K. Dreisewerd, The desorption process in MALDI, Chem. Rev. 103 (2003) 395–425.
[10] R. Knochenmuss, L.V. Zhigilei, Molecular dynamics model of ultraviolett matrix-assisted laser desorption/ionization including ionization processes, J. Phys. Chem. B 109 (2005) 22947–22957.
[11] R. Knochenmuss, L.V. Zhigilei, Molecular dynamics simulations of MALDI: laser fluence and pulse width dependence of plume characteristics and consequences for matrix and analyte ionization, J. Mass Spectrom. 45 (4) (2010) 333–346.
[12] M. Karas, M. Glückmann, L. Schäfer, Ionization in matrix-assisted laser desorption/ionization: singly charged molecular ions are the lucky survivors, J. Mass Spectrom. 35 (2000) 1–12.
[13] H. Ehring, M. Karas, F. Hillenkamp, Role of photoionization and photochemistry in ionization processes of organic molecules and relevance for matrix-assisted laser desorption ionization mass spectrometry, Org. Mass Spectrom. 27 (1992) 472–480.
[14] F.L. Brancia, M. Stener, A. Magistrato, A density functional theory (DFT) study on gas-phase proton transfer reactions of derivatized and underivatized peptide ions generated by matrix-assisted laser desorption ionization, J. Am. Soc. Mass Spectrom. 20 (2009) 1327–1333.
[15] X. Tang, M. Sageghi, Z. Olumee, A. Vertes, Matrix-assisted laser desorption/ionization by two collinear subthreshold laser pulses, Rapid Commun. Mass Spectrom. 11 (1997) 484–488.
[16] D.A. Allwood, R.W. Dreyfuss, I.K. Perera, P.E. Dyer, UV optical absorption of matrices used for matrix-assisted laser desorption/ionization, Rapid Commun. Mass Spectrom. 10 (1996) 1575–1578.
[17] V. Horneffer, K. Dreisewerd, H.-C. Lüdemann, F. Hillenkamp, F. Läge, K. Strupat, Is the incorporation of analytes into matrix crystals a prerequisite for matrix-assisted laser desorption/ionization mass spectrometry? A stucy of five positional isomers of dihydroxybenzoic acid, Int. J. Mass Spectrom. 185/186/187 (1999) 859–870.
[18] X. Chen, J.A. Caroll, R.C. Beavis, Near-ultraviolet-induced matrix-assisted laser desorption/ionization as a function of wavelength, J. Am. Soc. Mass Spectrom. 9 (1998) 885–891.
[19] D. Shannon Cornett, M.A. Duncan, I.J. Amster, Matrix-assisted laser desorption at visible wavelengths using a two-component matrix, Org. Mass Spectrom. 27 (1992) 831–832.
[20] D. Shannon Cornett, M.A. Duncan, I.J. Amster, Liquid mixtures for matrix-assisted laser desorption, Anal. Chem. 65 (1993), pp 2608-1613.
[21] X.K. Hu, D. Lacey, J. Li, C. Chang, A.V. Loboda, R.H. Ribson, Visible wavelength MALDI using Coumarin laser dyes, Int. J. Mass Spectrom. 278 (2008) 69–74.
[22] M.R. Papantonakis, J. Kim, W.P. Hess, R.F.Jr. Haglund, What do matrix-assisted laser desorption/ionization mass spectra reveal about ionization mechanisms, J. Mass Spectrom. 37 (2002) 639–647.
[23] K. Dreisewerd, M. Schürenberg, M. Karas, Matrix-assisted laser desorption/ionization with nitrogen lasers of different pulse widths, Int. J. Mass Spectrom. Ion Process. 154 (1996) 171–178.
[24] R. Knochenmuss, A. Vertes, Time-delayed 2-pulse studies of MALDI matrix ionization mechanisms, J. Phys. Chem. B 104 (2000) 5406–5410.
[25] M.W. Little, K.K. Murray, Two-laser mid-infrared and ultraviolet matrix-assisted laser desorption/ionization, Int. J. Mass Spectrom. 261 (2007) 140–145.
[26] P. Demirev, A. Westman, C.T. Reinmann, P. Hakanson, D. Barofsky, B.U.R. Sundquist, Y.D. Chen, W. Siebt, K. Siegbahn, Matrix-assisted laser desorption with ultra-short laser pulses, Rapid Commun. Mass Spectrom. 6 (1992) 187–191.
[27] J.M. Wichmann, C. Lupulescu, L. Wöste, A. Lindinger, Matrix-assisted laser desorption/ionization by using femtosecond laser pulses in the near-infrared wavelength regime, Rapid Commun. Mass Spectrom. 23 (2009) 1105–1108.
[28] M.J. Tomlinson, J.R. Scott, C.L. Wilkins, J.B. Wright, W.E. White, Fragmentation of an alkali metal-attached peptide probed by collision-induced dissociation fourier transform mass spectrometry and computational methodology, J. Mass Spectrom. 34 (1999) 958–968.
[29] J. Wichmann, C. Lupulescu, L. Wöste, A. Lindinger, Matrix assisted laser desorption/ionization of potassium adapted angiotensine II using femtosecond laser pulses, EPJD 52 (2009) 151–154.
[30] T.N. Laremore, R.J. Linhardt, Improved matrix-assisted laser desorption/ionization mass spectrometric detedtion of glycosaminoglycan disaccharides as cesium salts, Rapid Commun. Mass Spectrom. 21 (2007) 1315–1320.
[31] J. Zhang, E. Dyachovka, T.-K. Ha, R. Knochenmuss, R. Zenobi, Gas-phase potassium binding energies of MALDI matrices: an experimental and theoretical study, J. Phys. Chem. A 107 (2003) 6891–6900.
[32] J. Freeke, C.V. Robinson, B.T. Ruotolo, Residual counter ions can stabilise a large protein complex in the gas phase, Int. J. Mass Spectrom., doi:10.1016/j.ijms.2009.08.001.
[33] A.M. Weiner, Femtosecond pulse shaping using spatial light modulators, Rev. Sci. Instrum. 71 (2000) 1929–1960.
[34] X. Lou, J.L.J. van Dongen, J.A.J.J.M. Vekemans, E.W. Meijer, Matrix suppression and analyte suppression effects of quaternary ammonium salts in matrix-assisted laser desorption/ionization time-of-flight mass spectrometry, Rapid Commun. Mass Spectrom. 23 (2009) 3077–3082.
[35] M.V. Kosevich, O.A. Boryak, V.V. Chagovets, V.A. Pashynska, V.V. Orlov, S.G. Stepanian, V.S. Shelkovsky, Wet chemistry and crystollochemistry reasons for acidic matrix suppression by quaterny ammonium salts under matrix-assisted laser desorption/ionization conditions, Rapid Commun. Mass Spectrom. 21 (2007) 1813–1819.